THE JOURNAL OF PHYSICAL CHEMISTRY B
A JOURNAL OF THE AMERICAN CHEMICAL SOCIETY

pubs.acs.org/JPCB

Article

Transformation of Highly Stable Two-Component Glasses with Large T_g Contrast

Published as part of The Journal of Physical Chemistry B special issue "Robert Hamers Festschrift".

Megan E. Tracy,* Erik Thoms, Anthony Guiseppi-Elie, Ranko Richert, and Mark D. Ediger

Cite This: *J. Phys. Chem. B* 2025, 129, 6345−6356

Read Online

ACCESS | Metrics & More | Article Recommendations | Supporting Information

ABSTRACT: Physical vapor deposition (PVD) is a method of glass formation in which molecules utilize enhanced mobility at the free surface to reach highly equilibrated amorphous states. Codeposited glasses, made by simultaneously depositing more than one type of molecule onto the same substrate, are of technological and fundamental interest. Here, we use PVD to codeposit glasses of methyl-*m*-toluate (T_g = 170.0 K) and methyl acetate (T_g = 113.5 K), two molecules with extremely high contrast regarding their glass transition temperatures, T_g. For all compositions, we observe a delayed return to the equilibrium liquid when codeposited glasses are heated above the T_g of the mixture, as quantified by the onset temperature for the glass transition. When compared using normalized onset temperatures, the codeposited glasses have high kinetic stabilities that are only slightly lower than those of PVD glasses of the pure components. These results are readily interpreted if we assume that the surface mobility of the two components is similar during codeposition, despite the large ratio of T_g values for the pure components. Additionally, we deposit bilayer samples and measure the rate at which the lower T_g component dissolves glasses of the high T_g component for both highly stable and liquid-cooled glasses. Under these conditions, glass stability has little impact on the rate of dissolution.

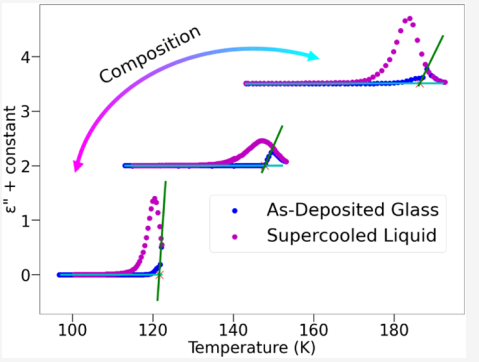

1. INTRODUCTION

Low molecular weight organic glasses are a class of disordered materials analogous to organic liquids, except that they are at such low temperatures that the molecules lack the mobility necessary to rearrange on the time scale of observation. As glasses, they are inherently out-of-equilibrium materials. During isothermal annealing, they continuously evolve toward the supercooled liquid in a process called structural recovery or physical aging.[1−5]

Despite their out-of-equilibrium status, glasses are useful materials for a variety of applications, including organic electronics[6−11] and pharmaceuticals.[12−18] For many applications, glasses with high density and low enthalpy are advantageous; molecular rearrangements in such materials are slow, and thus glass properties remain more consistent over time. High-density and low-enthalpy glasses are also of scientific interest, as they provide information about the ultimate properties of glasses and a potential thermodynamic transition to a new state of matter: the ideal glass.[19−25] Unfortunately, the preparation of such high-density and low-enthalpy glasses through traditional means would require thousands of years or longer.[23,26,27]

An alternative way to quickly make glasses with high density and low enthalpy was discovered in 2007.[28] This method involves physical vapor deposition (PVD), whereby molecules are deposited inside a vacuum chamber onto a substrate held at a temperature not far below T_g. The molecules are able to make use of enhanced mobility at the free surface[3,29−42] during deposition in order to quickly rearrange into configurations that are close to equilibrium for the temperature of the substrate and are then subsequently locked into that configuration by the arrival of further molecules onto the same surface. Reaching comparable density and enthalpy with a liquid-cooled glass through physical aging would take a very long time, with estimates typically falling into the range of hundreds to millions of years.[27,28,43] In comparison, PVD can form films with these properties in less than an hour.

High-density and low-enthalpy glasses have several unique characteristics that separate them from liquid-cooled glasses of the same materials, including high kinetic stability. When such glasses are heated continuously at a constant rate, they return to equilibrium more abruptly and do so at a higher temperature, characterized as an onset temperature, compared to their liquid-cooled counterparts.[2,19,28,44−48] Similarly, if a

Received: February 26, 2025
Revised: May 23, 2025
Accepted: June 2, 2025
Published: June 12, 2025

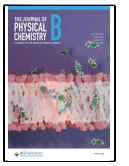

https://doi.org/10.1021/acs.jpcb.5c01326
J. Phys. Chem. B 2025, 129, 6345−6356

highly stable glass is annealed isothermally above T_g, it can take as long as 10^6 τ_α to return to equilibrium, where τ_α is the characteristic relaxation time for the supercooled liquid at that temperature. In contrast, liquid-cooled glasses subjected to the same thermal profile typically return to equilibrium in a few τ_α.[28] The onset temperature normalized to T_g and isothermal transformation times normalized to τ_α are commonly used to characterize and compare the stability of glasses.[49−51]

Further observation of a highly stable glass during its slow isothermal transformation to the liquid reveals a different mechanism of transformation in comparison to that of the liquid-cooled glass. Highly stable glasses initiate a growth front of supercooled liquid at the free surface due to the enhanced mobility.[48,49] These fronts of supercooled liquid propagate at a constant rate through the film, eventually transforming the entire sample. However, if the initiation of such a front is suppressed by a capping layer of a higher-T_g material, or if the film is thicker than a material-specific characteristic crossover length, a second, bulk, transformation mechanism will eventually intervene to transform the glass, relaxing the remaining material through the "nucleation" and growth of bubbles of supercooled liquid throughout the sample.[45,49,52−56] Highly stable glasses also resist other types of transformations beyond thermal rejuvenation. Chemical transformations of the molecules within the glass, initiated either by light[57,58] or by permeation of a gas,[17,59] proceed much more slowly in highly stable glasses compared to liquid-cooled glasses.

To date, fundamental work on PVD glasses has focused on films made of a single component. Codeposited glasses, mixtures formed by simultaneously depositing more than one component, are particularly relevant to applications in organic electronics. For example, in organic light-emitting diodes, typically an emitter molecule is codeposited with a host molecule; it has been shown that tailoring the deposition conditions of that mixed glass can improve the lifetime and efficiency of the device.[8,11,60] Previous work on codeposited mixtures has usually involved materials with similar T_g values,[61−63] sometimes even isomers of the same molecule,[48,64] or rather dilute regimes.[58] For a pair of materials with rather different T_g values codeposited onto the same substrate, the two types of molecules might be expected to have quite different surface mobilities. This has been observed in bulk systems for several so-called dynamically asymmetric mixtures, where the molecules have separated relaxation times and T_g values despite remaining well-mixed.[65−67] In a codeposition of two molecules with quite different T_g values, the surface equilibration mechanism might not be effective. One might imagine that stable glass formation would not be possible if only molecules of the lower T_g component had high surface mobility during deposition.

In this work, we codeposited two types of molecules, methyl-*m*-toluate (MMT) and methyl acetate (MeAc), that are structurally similar but have T_g values that differ by more than 50%. Codeposited glasses of all compositions showed high kinetic stability, similar to that observed for the pure components. Successful stable glass formation is consistent with the view that, during codeposition, the two components have similar surface mobilities, even for quite large T_g differences. Additionally, the transformation of the codeposited stable glasses shows both surface-initiated fronts and a bulk transformation mechanism, consistent with previous observations for single-component PVD glasses. Finally, the rates of dissolution of stable and liquid-cooled glasses of MMT into liquid MeAc were compared.

2. METHODS

2.1. Vapor-Deposited Samples. Liquid samples of methyl-*m*-toluate (MMT, 98%, 150.18 g/mol, 1.062 g/mL, T_g = 170.0 K) and methyl acetate (MeAc, 99%, 74.08 g/mol, 0.934 g/mL, T_g = 113.5 K, as established below) were purchased from Alfa Aesar and Thermo Scientific, respectively, and were each used as received. Vapor deposition took place within a custom-built vacuum chamber with a characteristic base pressure below 10^{-9} Torr, as has been described previously.[2,19,37,47,48,68−70] The temperature of the substrate was controlled by competition between cooling from a liquid-nitrogen-filled cold cup and heating from a cartridge heater near the substrate. The temperature was monitored continuously by a three-wire RTD near the substrate, which was accurate to within 0.5 K based on a comparison of dielectric spectra of the supercooled liquid of MMT with literature data.[50,71]

Stainless-steel crucibles containing MMT and MeAc were attached to the exterior of the deposition chamber through, first, a gate valve and then a fine leak valve. Deposition rates were set for each component independently prior to each codeposition. This method resulted in a small layer of nearly pure MMT (less than 15 nm) at the top and bottom of each (>5 μm) film. Total deposition rates were in the range of 1−3 nm/s, depending on the target composition; MMT-rich mixtures were on the lower side, while MeAc-rich mixtures were on the higher side of this range. A variety of target compositions was chosen such that the range from 6 to 97% MMT by volume was explored. For each composition regime (majority MeAc, roughly 50/50 MMT:MeAc, and majority MMT), a range of deposition temperatures was chosen to explore the stability of the glasses formed.

Films of all compositions were deposited onto an IME 1025.3-FD-Pt-U interdigitated electrode (IDE) cell manufactured by ABTECH Scientific, Inc., which has been described previously.[68] The cell features two independent capacitors (C_{geo} = 0.65 pF), each with a 10 μm digit width and interdigit spacing. This allowed dielectric measurements to be conducted *in situ* before, during, and after the deposition of each film. One set of electrodes was exposed to deposition, collecting the sample film on their active surface, while the other set was kept covered to allow a simultaneous reference measurement of the bare substrate. After deposition was completed, the chamber was backfilled with dry nitrogen gas to ∼100 Torr to prevent desorption during the rest of the experiment.

Dielectric permittivities were measured using two transimpedance amplifiers and a Solartron SI-1260 impedance analyzer.[72,73] Permittivities at a frequency of 20 Hz were recorded during ramping experiments to measure onset temperatures, using a heating rate of 5 K/min. Dielectric spectra measured at a constant temperature were also acquired using a range of frequencies from 0.1 to 10^5 Hz. Although this has no impact on any of the conclusions presented in this article, we note that the dielectric permittivities reported here for thin films are not independent of the sample geometry. Our films are not thick enough to fill the entire measurement region of the IDE, and thus the measured values are lower than the true values (just as they would be in a partially filled parallel plate capacitor). The dielectric permittivities reported here

https://doi.org/10.1021/acs.jpcb.5c01326
J. Phys. Chem. B 2025, 129, 6345−6356

depend upon film thickness, as described in previous work.[36,48,68]

Two temperature protocols were used to characterize the codeposited glasses. Temperature-ramping experiments (5 K/min) were used to determine the onset temperature for the transformation of the glass (monitored at 20 Hz). The resulting supercooled liquid was cooled below T_g and then heated to determine the 20 Hz T_g (where the loss measured at 20 Hz goes through a maximum) for the liquid-cooled mixed glass. A second temperature protocol, isothermal transformations, was performed by ramping the film at a rate of 20 K/min from the deposition temperature to the annealing temperature. The dielectric constant was monitored at a pair of frequencies during annealing until it reached a constant value. Additionally, two full dielectric spectra were recorded at the annealing temperature upon the conclusion of the transformation to characterize the τ_α of the mixture at that temperature. After the transformation was completed, the experimental 20 Hz T_g was recorded for each film on cooling to the liquid.

2.2. Bulk Samples. For comparison with the vapor-deposited samples, bulk mixtures of MMT (Acros Organics, 99%, distilled) and MeAc (Sigma-Aldrich, 99.5%) were prepared with MMT concentrations of ∼20 to 100% by weight, using a microbalance scale to determine composition (bulk samples of neat MeAc could not be studied due to crystallization). To inhibit a change in composition due to differential evaporation of the components, the samples were kept in closed containers and processed rapidly. To facilitate mixing, MMT:MeAc samples were subjected to an ultrasonic bath for a minimum of 1 min. All samples were clear, colorless liquids, and no visible signs of component segregation were observed in exemplary samples after 24 h at room temperature. As an additional test of miscibility, a set of 2 mL samples of selected compositions (0%, 10%, 33%, 50%, 66%, 90%, and 100% MMT by volume; MMT from Alfa Aesar and MeAc from Thermo Scientific) were prepared and stored for several days at 195 K to test miscibility at lower temperatures. Visual observation confirmed that these samples remained well-mixed liquids throughout that time, with the exception of the 90% and 100% MMT samples, which crystallized at this temperature.

For each of the bulk MMT:MeAc mixtures, a parallel plate capacitor (stainless steel, diameter = 16 mm, plate separation = 180 μm) was filled with the sample and immediately sealed before being placed in a cryostat (Novocontrol Quatro, temperature resolution ΔT = 0.1 K). To avoid crystallization, the sample cell was rapidly cooled to below the glass transition temperature of the sample. Dielectric spectra were captured at selected temperatures during heating, with a minimum of 5 min of stabilization time at each temperature, utilizing a Solartron SI-1260 frequency response analyzer with a Mestec DM-1360 transimpedance amplifier.

These bulk measurements provided a determination of the 20 Hz T_g values as a function of composition, which were used to determine the actual composition for each vapor-deposited sample. The actual composition determined by this route typically agreed with the target composition based on the deposition rates within ∼10%.

3. RESULTS: REFERENCE DIELECTRIC MEASUREMENTS ON NEAT MEAC AND BULK MIXTURES OF MMT:MEAC

To allow better interpretation of the results obtained for codeposited glasses of MMT:MeAc, we first conducted experiments on neat MeAc films and bulk mixtures across the range of compositions. Dielectric spectroscopy results for neat MMT have been previously published.[68]

3.1. Supercooled Liquid of Neat MeAc. Due to the difficulty of avoiding crystallization of MeAc upon cooling from the bulk liquid, we studied glasses and supercooled liquids of MeAc formed through vapor deposition. Deposition of neat MeAc below T_g resulted in the formation of stable glasses for a wide range of deposition temperatures; these results will be summarized below. In this section, we focus on the properties of the supercooled liquid of MeAc that was formed by heating PVD glasses above T_g.

The top panel of Figure 1 shows dielectric loss spectra obtained for the supercooled liquid of MeAc at temperatures from 114 to 121 K. For the 120 and 121 K cases, it is apparent that the sample started to crystallize. The characteristic relaxation time for each temperature, which we will refer to as τ_α for this analysis, was calculated from the frequency at

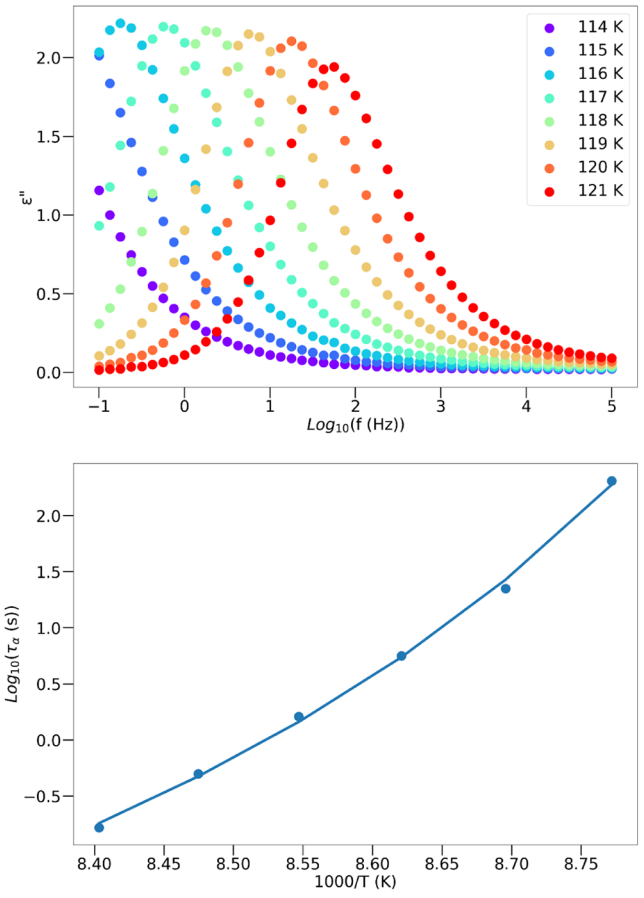

Figure 1. Top: Dielectric loss spectra were obtained for the supercooled liquid of MeAc. A single spectrum was collected at each temperature. The highest two temperatures, 120 and 121 K, showed a loss of intensity due to crystallization and were not included in further analysis. Bottom: VFT fit to the extracted τ_α values as a function of inverse temperature, with parameters A = −6.92, B = 74.90 K, and T_0 = 105.08 K.

https://doi.org/10.1021/acs.jpcb.5c01326
J. Phys. Chem. B 2025, 129, 6345−6356

which the maximum loss occurs: $\tau_\alpha = 1/(2\pi f_{max})$. The second panel of Figure 1 shows a fit of $\log(\tau_\alpha/s)$ as a function of inverse temperature, using the Vogel–Fulcher–Tammann (VFT) function, $\log_{10}(\tau_\alpha/s) = A + B/(T - T_0)$. By extrapolation, this analysis gave a T_g value (where τ_α = 100 s) of 113.5 K for MeAc. As far as we are aware, this is the first time that a T_g value has been reported for neat MeAc.

3.2. Bulk Mixtures of MMT:MeAc. A parallel plate capacitor was used to obtain dielectric data for bulk mixtures of six different compositions (23%, 38%, 54%, 68%, 81%, and 83% MMT by weight), as well as for neat MMT (100%) at various temperatures near T_g. The dielectric loss spectra are presented in Figure S1. The frequency of maximum loss was used to determine values of τ_α as a function of temperature, as described above. These τ_α values are displayed in Figure 2A, along with fits based on the VFT function. The parameters for the VFT fits are provided in Table S1.

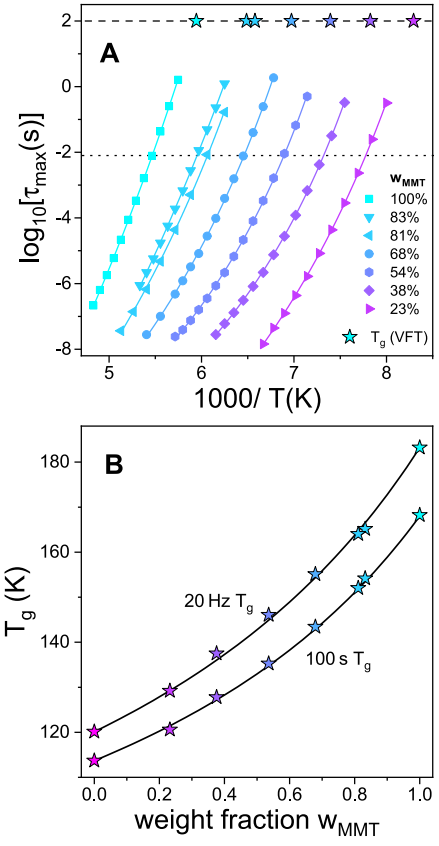

Figure 2. (A) Values for τ_α as a function of inverse temperature for a series of bulk mixtures of MMT and MeAc with the indicated compositions. Solid lines are fits using VFT functions, and levels corresponding to 20 Hz and 100 s T_g values are shown as dotted and dashed lines, respectively. (B) T_g values as a function of composition for bulk mixtures of MMT:MeAc. T_g values for neat MeAc from thin-film experiments are included as the lower end point. The solid black curves represent fits using the Gordon–Taylor function with k = 0.56.

We used the data in Figure 2A to extract the T_g values as a function of composition. Figure 2B shows both the 20 Hz T_g and the more traditional T_g defined by τ_α = 100 s; these two quantities are both important for later analyses. Both sets of T_g values were fitted by a Gordon–Taylor function[74] as a function of the weight fraction of MMT:

$$T_g(w_{MMT}) = \frac{(1 - w_{MMT}) \times T_{g,MeAc} + k \times w_{MMT} \times T_{g,MMT}}{((1 - w_{MMT}) + k \times w_{MMT})}$$

Here, w_{MMT} is the weight fraction of MMT, and $T_{g,MMT}$ and $T_{g,MeAc}$ are the T_g values of the neat materials. A k value of 0.56 provided the best fit to both the 20 Hz T_g and 100 s T_g values, and this function was used to determine the composition of all vapor-deposited samples based on their T_g values.

4. RESULTS

4.1. Stability of Vapor-Deposited Glasses of MMT:MeAc Mixtures and the Pure Components: Onset Temperatures. Figure 3 shows representative

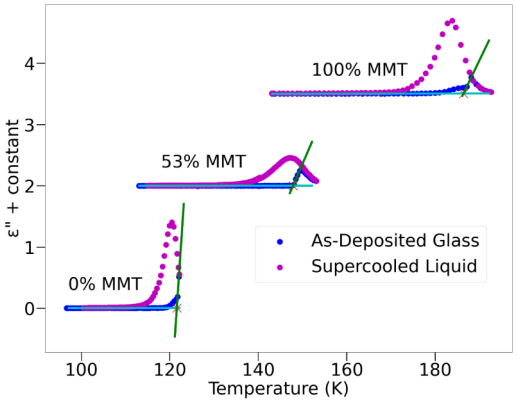

Figure 3. Dielectric response of vapor-deposited glasses (blue points) obtained during heating and the response of the supercooled liquid (purple points) obtained during subsequent cooling. Dielectric data are shown at 20 Hz during ramping of three compositions: neat MeAc (lower left, deposited at 0.85T_g), a codeposited mixture of 53% MMT (middle, deposited at 0.77T_g), and neat MMT (upper right, deposited at 0.80T_g). Loss curves for 53% and 100% were, respectively, shifted vertically by 2.0 and 3.5 to allow comparison. The lines indicate the determination of the onset temperature for the transformation of the as-deposited glass into a supercooled liquid. The cyan line is the fit to the low temperature, i.e., glassy loss, while the green line is the fit to the transformation regime. The red × marks their intersection which defines the onset temperature.

dielectric loss data for a vapor-deposited glass of MeAc (0% MMT) deposited at 0.85T_g. The blue points show the data obtained for the as-deposited glass at 20 Hz, with increasing temperature at a rate of 5 K/min. At about 121 K, the loss increases sharply, indicating the onset of transformation to the supercooled liquid. In order to obtain consistent onset temperatures for glasses of different stabilities and compositions, two straight lines were fitted to different regions of the data, as illustrated in Figure 3: the first in the low-temperature (glassy) range and the second in the higher-temperature range (mid-transformation, capturing the bulk process rather than the surface process, which begins first). The intersection of these two lines is a characteristic temperature for the start of the bulk transformation process. This same procedure was previously utilized for vapor-deposited glasses of neat MMT.[68] Also shown in Figure 3 are representative data for a vapor-deposited glass of neat MMT (deposited at 0.80T_g) and for a codeposited glass (53% MMT, deposited at 0.77T_g).

https://doi.org/10.1021/acs.jpcb.5c01326
J. Phys. Chem. B 2025, 129, 6345–6356

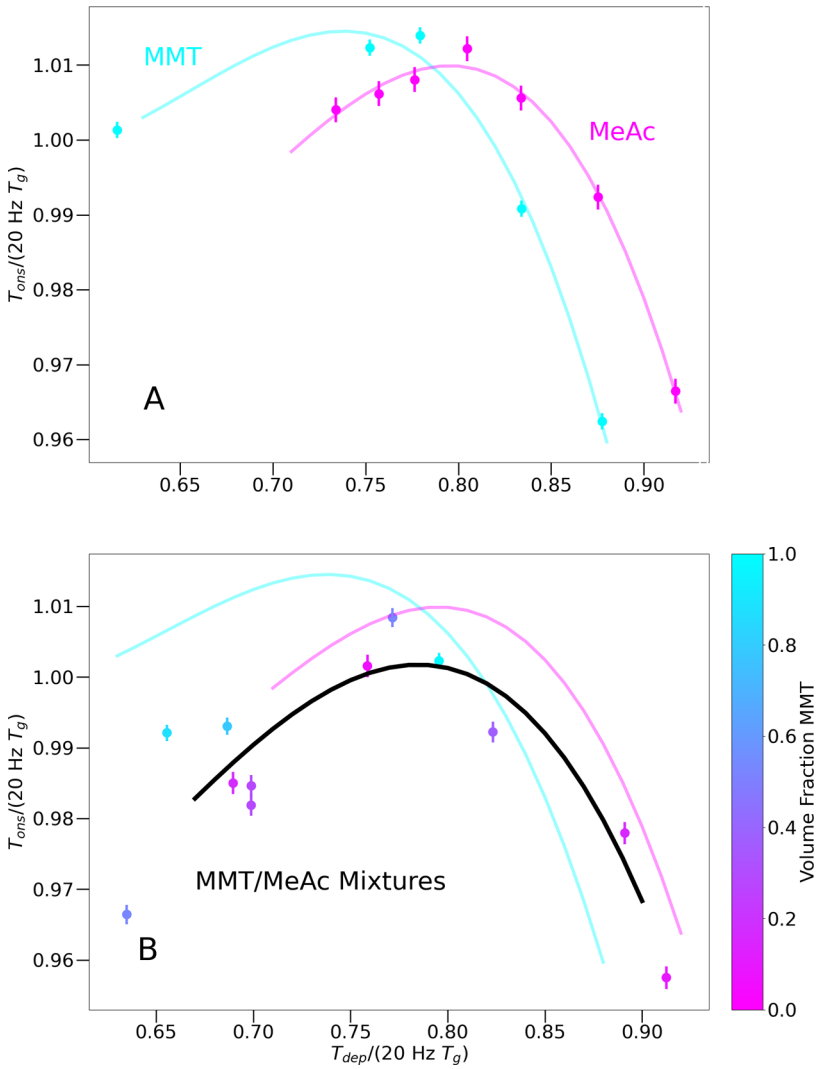

Figure 4. Normalized onset temperature as a function of normalized deposition temperature for stable vapor−deposited glasses of neat MMT (cyan circles), neat MeAc (magenta circles), and codeposited mixtures (circles colored according to relative composition). Lines are guides for the eye. (A) Neat MeAc and neat MMT glasses only. (B) Data for the codeposited mixtures, with the pure component trends included for reference.

For all three data sets in Figure 3, after the complete transformation of the initially prepared stable glass, dielectric data of the supercooled liquid were obtained by cooling the sample at 5 K/min (purple points). The temperature of maximum of the purple data points is 20 Hz T_g. The delayed dielectric response of the as-deposited glass relative to the supercooled liquid is a direct measure of the high kinetic stability of the as-prepared glasses.

A convenient way to compare the stabilities of different vapor-deposited glasses is shown in Figure 4. In both panels, the *y*-axis is the onset temperature divided by the 20 Hz T_g; this is a normalized measure of the kinetic stability of the as-deposited glass. In both panels, the *x*-axis is the substrate temperature normalized to the 20 Hz T_g; this reduced substrate temperature has been shown to be the most important parameter in determining the stability of vapor-deposited glasses.[28,75]

Figure 4A compares the kinetic stabilities of the vapor-deposited glasses of the two pure components. Qualitatively similar results are observed for MMT and MeAc glasses. In both cases, the kinetic stability is maximized for deposition near 80% of 20 Hz T_g. As discussed in previous work, kinetic stability at higher substrate temperatures is limited by the low thermodynamic driving force, while kinetic stability at lower substrate temperatures is limited by the lack of sufficient surface mobility. The maximum stability occurs at a temperature where equilibration can substantially enhance stability, and surface mobility is sufficient to allow substantial equilibration.

Figure 4B adds kinetic stability data for codeposited glasses to the results for the pure components (now represented only by the trend lines), using the same axes scaling as Figure 4A. All the codeposited samples are represented by stars, with the color of the star indicating the composition of the mixture. The solid black curve shows the trend of the stability data for the codeposited glasses. The codeposited glasses all follow the same stability trend with deposition temperature as the neat materials, regardless of composition. This suggests that the surface equilibration mechanism that describes single-component stable glass formation is also responsible for the stability of the MMT:MeAc mixed glasses.

As a note, this stability data for the codeposited glasses of MMT:MeAc is presented in Figure 4 in an unconventional format, requiring some additional explanation. In previous

https://doi.org/10.1021/acs.jpcb.5c01326
J. Phys. Chem. B 2025, 129, 6345−6356

work on vapor-deposited glasses, the 100 s T_g value has been conventionally used for normalization; this is in contrast with the 20 Hz T_g values utilized for normalization in Figure 4. We chose the 20 Hz values in this figure because these are either directly measured (for vapor-deposited glasses) or readily available via interpolation (for the reference data shown in Figure 2A). In contrast, the 100 s T_g values for these samples are available only by extrapolation, which necessarily involves additional error in the plot. Since these values are useful for comparisons with other published work on single- and multicomponent PVD glasses, we perform this extrapolation in order to report the conventionally normalized values for the same data presented in Figure 4, shown in Figure 5.

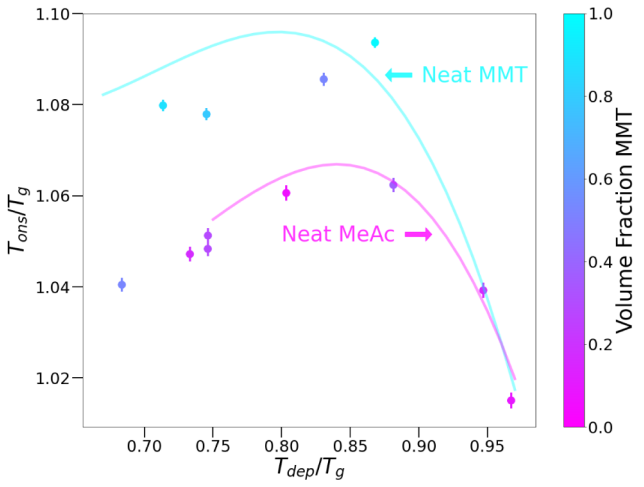

Figure 5. Onset temperatures for codeposited glasses of MMT and MeAc (circles, colored according to relative composition) as a function of deposition temperature, with both axes normalized to their respective 100 s T_g values. Onset temperatures for glasses of neat MMT and MeAc are represented by the solid-colored trend lines.

The representation of the stability data in Figure 5 allows us to make several important comparisons. For all of the samples, the most stable glasses have T_{on}/T_g values in the range of 1.06−1.09. This is the same range observed previously for highly stable single-component glasses,[47,48,68−70,76] so we conclude that codeposited mixtures of MMT:MeAc show very high kinetic stability. We note that the neat MMT and MeAc glasses show two distinct trends with the deposition temperature, in contrast to the very similar trends shown for the 20 Hz T_g data in Figure 4. This different appearance of the two figures is due to the difference in the fragilities of the liquids. MMT is a strong glass-forming liquid, meaning that the temperature dependence of its relaxation times is close to Arrhenius behavior. MeAc, on the other hand, is a more fragile glass-forming liquid, and its relaxation times are more strongly dependent on temperature. Figure 4 more accurately compares the stabilities of the neat glasses because the onset temperature is approximately equal to the 20 Hz T_g. We note in Figure 5 that mixed stable glasses closer in composition to pure MeAc have stabilities similar to neat MeAc glasses, while those mixed glasses closer in composition to pure MMT are more similar to neat MMT glasses; this feature is also related to the different fragilities of the mixtures; see Table S1.

4.2. Stability of Vapor-Deposited Glasses of MMT:MeAc Mixtures: Isothermal Transformation. In addition to the temperature-ramping experiment described above, stable codeposited glasses were also transformed isothermally. Isothermal transformation allows for the measurement of the transformation time, which is a very direct characterization of kinetic stability. In addition, as will be discussed below, such experiments allow for the identification of surface and bulk contributions to the transformation.

Figure 6 shows a typical experiment in which both the real and imaginary values of the complex dielectric permittivity

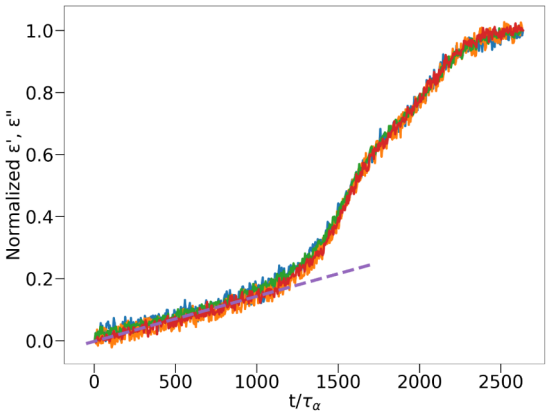

Figure 6. Real (blue and green) and imaginary (orange and red) components of the dielectric response measured at 8 and 42.17 Hz, respectively, during the isothermal transformation of a mixed stable glass at 124 K. The glass sample was 700 nm thick and 19.3% MMT by volume, deposited at ∼0.85T_g. Deposition was conducted so that the film was not capped by MMT at the free surface. The violet dashed line is a fit to the region where the surface-initiated growth front mechanism is dominant.

were monitored at two different frequencies during the isothermal transformation of a stable codeposited glass; these values are normalized to their initial and final values to reflect only the change due to the transformation from the stable glass to the supercooled liquid. The x-axis in Figure 6 is time expressed in units of τ_α at the experimental temperature. As shown in the figure, the four dielectric quantities superpose well, which is consistent with a two-state picture of the transformation. That is, at any given time, all the material contributing to the dielectric response is either in the stable glass state or in the supercooled liquid.[77]

The data in Figure 6 show two transformation regimes. At short times, the transformation proceeds linearly, as shown by the fit represented by the violet dashed line. Based upon previous work on single-component systems, we interpret this to indicate that a front of supercooled liquid is growing into the stable glass from the free surface at a constant velocity.[45,48,49,78−81] The velocity of the growth front is about 0.1 nm/τ_α, which can be expressed as roughly 0.15 molecular diameters/τ_α. Previous work has shown that fronts propagate even more slowly in the most stable single-component PVD glasses, ∼0.02 molecular diameters/τ_α, and the value obtained here would indicate that this codeposited glass of MMT:MeAc is moderately stable.[45,50,56,69,82] At times longer than about 1300 τ_α, the transformation shown in Figure 6 occurs more rapidly than was expected for the surface transformation front. Based upon previous work on single-component systems, we interpret this as a bulk transformation process in which bubbles of supercooled liquid are formed and then grow in the interior of the film.[45,50,55,56,78,79,83]

https://doi.org/10.1021/acs.jpcb.5c01326
J. Phys. Chem. B 2025, 129, 6345−6356

We can further test the transformation mechanism for the codeposited stable glasses of MMT:MeAc by manipulating the deposition procedure. In Figure 7, we show an isothermal

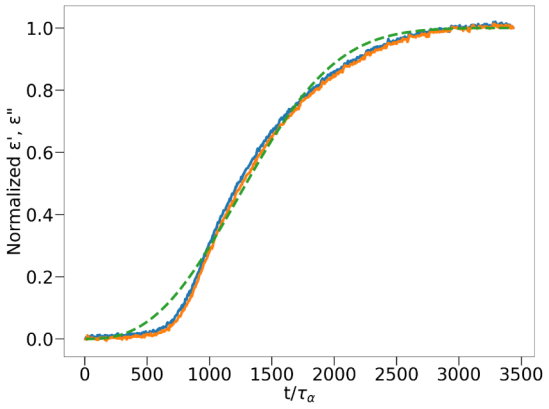

Figure 7. Normalized real (blue) and imaginary (orange) components of the dielectric response measured at 20 Hz during isothermal transformation of a 2.4 μm thick glass that is 31% MMT by volume during annealing at 129 K. This film was deposited at ~0.82T_g. The green dashed line is a fit to the real component using the Avrami model with $K = 4.71 \times 10^{-9}$ s^{-1} and $m = 2.62$. The fit to the imaginary component (not shown) is essentially the same shape.

transformation experiment on another codeposited glass. For comparison, this sample is thicker than the one studied in Figure 6 and is also capped by a thin layer of MMT. Both of these changes are expected to suppress the surface-initiated transformation during isothermal annealing.[48,78,84] Consistent with this expectation, essentially no initial linear transformation process is observed in Figure 7. The sigmoidal shape of the transformation curve is qualitatively consistent with previous work on single-component stable glasses;[45,48,55,68,85] we return to this point below. The transformation shown in Figure 7 required roughly 3000 τ_α to complete. In comparison to previous work on single-component systems, this value indicates that this glass is reasonably stable, if somewhat less stable than the most stable glasses ever reported (which can take times in excess of 10^6 τ_α).[45,49,53,78,79,82] For further context, we note that liquid-cooled glasses typically have transformation times of a few τ_α.

We use the Avrami model[86] to analyze the transformation in Figure 7 more quantitatively:

$$Y(t) = 1 - e^{-Kt^m}$$

Here, Y is the fraction of material transformed as a function of time (t), and K and m are the fitting parameters. The value of the exponent m can be used to gain physical insight into the mechanism of transformation. Figure 7 shows an Avrami fit to the experimental data as a dashed line, which indicates a value of $m = 2.6$. Clearly, this fit does not provide a very good description of the data. If only the first portion of the data is fit, up to 1000 τ_α, this first part of the transformation can be well described with $m = 4.8$. In the Section 5, we put this result into the context of recent work.

4.3. Dissolution of Glasses of MMT in Liquid MeAc.

Given the miscibility of liquids of MMT and MeAc across all tested compositions, it is of interest to observe the rate of dissolution of MMT glass in MeAc. Specifically, we wanted to test whether stable glasses of MMT dissolved more slowly than liquid-cooled glasses in MeAc. Based on previous work in which various perturbations were used to disrupt stable glass packing (including temperature, gas permeation,[17,59] and light[57,58]), we expected the stable glass to be significantly more robust against dissolution. However, the experimental results do not support this expectation, as shown below.

To perform this experiment, bilayer samples were formed. A ~200 nm layer of either highly stable or liquid-cooled MMT was prepared on the substrate, and then an ~200 nm stable glass of MeAc was deposited on top. To characterize the dissolution process, the temperature of each sample was cycled twice. The initial heating ramp was performed at 20 K/min to avoid crystallization of MeAc, and then subsequent heating and cooling were performed at a rate of 5 K/min.

Figure 8 shows results for temperature cycling of the bilayer samples using dielectric storage at 20 Hz to monitor the

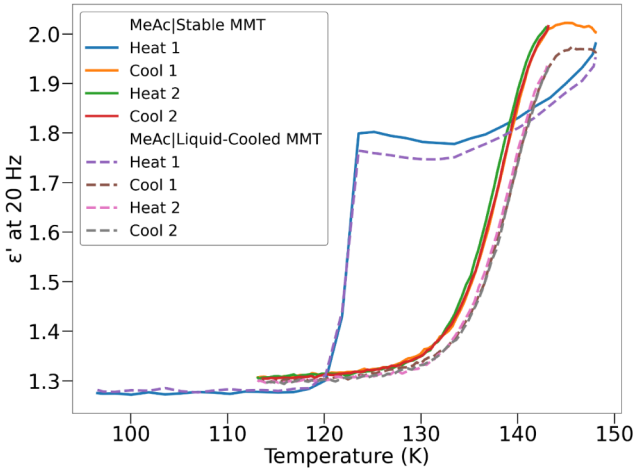

Figure 8. Dissolution of the MMT glasses into the MeAc liquid. Two bilayer experiments are shown in which a stable glass of MeAc is deposited upon either a stable glass or a liquid-cooled glass of MMT. The y-axis shows the dielectric storage signal at 20 Hz measured during temperature cycling of the samples. The bilayer with a stable glass of MMT is represented by solid lines, while the bilayer with the liquid-cooled glass of MMT is represented by dashed lines. No normalization was performed to force alignment of these data.

transformation process. Since MMT and MeAc have similar dipole moments, the magnitude of the storage is roughly proportional to the number of dipoles that are mobile (relative to the 20 Hz detection frequency). The major features of these experiments are described as follows. During the initial heating, a sharp increase in the storage is observed near 122 K; based upon other experiments, this is the transformation of the stable glass of MeAc into the supercooled liquid of MeAc. The next feature observed in the initial heating is a gradual increase in the magnitude of the storage starting just above 130 K; we understand this to result from the dissolution of MMT glass into MeAc. After the temperature ramp was reversed at 147 K, the storage signal continues to increase until about 143 K; this indicates continued dissolution of MMT into MeAc. Below 143 K, the signal decreases upon cooling; we interpret this as the dynamic glass transition (at 20 Hz) for the now-mixed liquid of MeAc and MMT, with no further dissolution upon cooling. Consistent with this interpretation, the second heating/cooling cycle reproduces the cooling data from the first cooling cycle. The dynamic glass transitions (near 137 K for both experiments) can be used to infer that the average composition of the mixed liquids at the end of the experiments

https://doi.org/10.1021/acs.jpcb.5c01326
J. Phys. Chem. B 2025, 129, 6345−6356

is about 40% MMT, indicating that some unmixed MMT may be present at the end of the experiment, i.e., the dissolution may not be complete.

It is clear from Figure 8 that the mixing of MMT and MeAc in the two samples is nearly identical, regardless of whether the underlayer of MMT was a stable or liquid-cooled glass. If we examine the data closely, for the bilayer with the liquid-cooled glass of MMT, the transformation begins at a slightly lower temperature (133.1 K compared to 133.7 K, with a difference that is at the edge of our temperature resolution) and with a slightly higher slope. While this suggests that the stable glass of MMT may require slightly more time to dissolve in the MeAc liquid, there is certainly no evidence that the stable glass dissolves substantially more slowly. We discuss possible interpretations of this result below.

While conducting these bilayer experiments, some additional experiments were performed where bilayer samples were annealed at temperatures above the glass transition temperature of MeAc but below that of MMT. Surprisingly, the supercooled liquids of MeAc showed different rates of crystallization depending on the stability of the underlying MMT glass. While this phenomenon was not explored in detail, we have included these experimental results in Figure S2.

5. DISCUSSION

In this paper, we show that codeposited glasses of MMT and MeAc have all the features previously observed for highly stable glasses of single-component systems, in spite of the 50% difference in T_g values for the neat components. For these mixed glasses, the onset temperature for transformation into the supercooled liquid depends upon substrate temperature in the same manner as observed for single-component systems, with the most stable glasses obtained for deposition at temperatures near $0.85T_g$. Based on the normalized onset temperatures, the mixed glasses of MMT:MeAc are as stable as the pure components. During isothermal transformation, codeposited glasses of MMT and MeAc show evidence of both surface-initiated and bulk transformation processes that are qualitatively similar to those of single-component stable glasses. The isothermal transformation time is observed to be ~3000 τ_α, a value indicating reasonably high stability. Surprisingly, we find no difference between the rate of dissolution for stable and liquid-cooled glasses of MMT when MeAc is the solvent. In this section, we discuss the implications of all of these findings.

5.1. Extension of the Surface Equilibration Mechanism to a Mixed System with Large T_g Ratio. The kinetic stability demonstrated by these codeposited glasses and its trend with deposition temperature suggest that the same mechanism governs the stable glass formation during deposition for both mixed and neat glasses. For single-component systems, stable glass formation is well described by the surface equilibration mechanism. Mobility at the free surface of an organic glass can be many orders of magnitude higher than in the bulk, and during deposition, this mobility leads to rapid equilibration. A few studies of codeposited glasses are also consistent with the surface equilibration mechanism,[8,48,58,61−64] although in these cases, the ratio of the T_g values for the two components was relatively small, in the range of 1.0−1.15. For MMT:MeAc, the ratio of T_g values is 1.5, and experiments on this system test the surface equilibration mechanism in a new regime.

It is somewhat surprising that the surface equilibration mechanism works well for MMT:MeAc. Because of their different T_g values, surface mobility for the neat materials at any common temperature would be expected to be quite different, and these differences might well be present at the surface of the mixed glass. For example, while deposition at 100 K yields a highly stable glass of MeAc, only a moderately stable glass of MMT is formed at this temperature.[2,45,68] From this result, we infer that surface mobility at 100 K is very high on neat MeAc, while it is likely much smaller on neat MMT. One might imagine that codeposition at 100 K would not yield a stable glass if the slow mobility of MMT were to limit equilibration.

The observation that very stable mixed glasses can be formed for deposition near 100 K argues for an alternate picture: On a mixed surface, the two types of molecules may have similar surface mobilities, roughly the average of the surface mobilities of the two pure components at that temperature. The averaged mobility would have a temperature dependence similar to that of the neat materials when normalized to their respective T_g values, allowing all molecules at the surface to rearrange quickly before they are buried, regardless of their chemical identity. This view of averaged surface mobility has not been directly tested in experiments, to our knowledge, but it has been previously articulated to explain stable glass formation via codeposition of components with more similar T_g values.[48,61,62,64,87] The idea that component mobilities would be highly averaged at the surface is analogous to the averaging of bulk mobilities in MMT:MeAc mixtures, as evidenced by the lack of distinct peaks in the loss spectra (Figure S1). This idea is consistent with the theoretical approach of Stevenson and Wolynes, who describe surface mobility as a cooperative process that involves many molecules at and near the surface.[35]

We are optimistic that our results can be generalized to other mixtures, in which the components have significantly different T_g values. This may find applicability in the field of organic electronics.

5.2. Isothermal Transformation of Stable Codeposited Glasses. As shown in Figures 6 and 7, the isothermal transformation times for mixed MMT:MeAc glasses exceed 10^3 τ_α, as expected for the formation of quite stable glasses (though transformation times exceeding 10^5 τ_α have been observed for some single-component stable glass systems). In previous work, the Avrami exponent m has been used to discuss the mechanism of transformation into the supercooled liquid. If thick films (or capped films) are utilized, then the surface-initiated transformation mechanism is suppressed, and, in principle, the Avrami exponent can be used to understand the bulk transformation mechanism.

We briefly summarize some of the published isothermal transformation experiments as context for our current results. Kearns et al.[85] used nanocalorimetry to characterize the transformation of thick stable glasses of indomethacin, with the data reasonably described with an Avrami exponent $m \approx 4$; the exponent is consistent with random three-dimensional nucleation of bubbles of supercooled liquid inside the stable glass, followed by the growth of these bubbles in three dimensions. Note that "nucleation" is used here as a phenomenological description that does not imply the existence of a true phase transition. Vila-Costa et al.[83] used nanocalorimetry to study both thin (capped) and thick films of stable indomethacin glasses, finding a good description of the

https://doi.org/10.1021/acs.jpcb.5c01326
J. Phys. Chem. B 2025, 129, 6345−6356

data with Avrami exponents of 2 and 3, respectively. These results were interpreted in terms of instantaneous nucleation of supercooled liquid bubbles, followed by constant velocity growth in either two or three dimensions.

Most relevantly, Kasting et al.[48] used dielectric relaxation to characterize the transformation of stable glasses of *trans*-decahydroisoquinoline, as well as mixtures of the *cis*- and *trans*-isomers. The *trans*-isomer was well described with an Avrami exponent $m \approx 9$; the Avrami scheme does not offer a simple interpretation of such a large exponent. Kasting et al. also reported that the transformation of stable glasses of mixtures of *cis*- and *trans*-decahydroisoquinoline was not well fit by the Avrami model, with the best fit having $m = 2.5$; their mixed isomer results were qualitatively similar to those shown for MMT:MeAc mixed glasses in Figure 7.

Recent computer simulations offer an explanation for nonstandard Avrami exponents and more generally for transformation curves that cannot be fit with the Avrami model. Herrero et al.[55] used molecular dynamics simulations to analyze the kinetics of the isothermal transformation of a stable glass formed using Swap Monte Carlo. These results clearly show the nucleation of small bubbles of supercooled liquid, followed by their growth and ultimately by their coalescence. The bubbles are initially under pressure because the supercooled liquid is less dense than the surrounding stable glass; this pressure slows liquid dynamics, which in turn slows the growth of bubbles. After coalescence, the supercooled liquid pressure drops to ambient pressure, causing the liquid dynamics to become faster and the growth rate to increase. This variation of the growth rate over time violates a key assumption used to derive the Avrami equation. Thus, when the simulation results are fit to the Avrami form, the fits are imperfect, and the apparent exponents are too large for any standard explanation.

We are not able to find a simple explanation for our new experimental results in the context of these simulations or the previous experiments. We see no reason to question the existence of the surface-initiated transformation process apparent for thin films (Figure 6) or the bulk transformation process, which is dominant in thick films (Figure 7). The simulations explain how large m values might arise, but further work is needed to understand why they are only observed for a subset of experimental systems. Composition fluctuations in a mixed, as-deposited glass might possibly change the transformation kinetics; such a possibility is consistent with work by Wolynes, who indicated that the stretching exponent that characterizes the supercooled liquid will influence the transformation process.[88] At this point, from the experiments, it is unclear whether mixtures and single-component stable glasses show transformation curves of systematically different shapes.

5.3. Dissolution of MMT Glasses in Liquid MeAc. In the experiment shown in Figure 8, the stable glass of MMT appears to be only marginally more resistant to dissolution into the MeAc liquid on heating in comparison to the liquid-cooled glass. We found this to be surprising, given previous results showing that the isothermal transformation rate (glass to supercooled liquid) of a single-component stable glass is of 10 orders of magnitude slower than that of the liquid-cooled glass.[45,48,49,52−56,83] In addition, the isothermal transformation rate decreases by about a factor of 10 when transitioning from a moderately stable to a highly stable glass.[80,82] These results have been rationalized by invoking the higher energy barriers associated with efficient packing in stable glass. We envision that these higher barriers should also play a role when stable glass is dissolved by a solvent. Indeed, previous results from Smith et al. support this conclusion.[59] These authors measured the permeation of krypton (Kr) (the "solvent" in this analogy) into PVD glasses of toluene of varying stability. For highly stable glasses, permeation is only observed above the onset temperature for the transformation of the stable glass into the supercooled liquid; Kr can move ∼100 nm into a low-stability glass while moving ∼0 nm into a stable glass. Although the Kr concentration in these experiments was too low to characterize "dissolution" of toluene, these results strongly support the view that the initial stages of dissolution can be significantly slowed by a stable glass.

So why do the results in Figure 8 show very little difference between the dissolution of stable and liquid-cooled glasses of MMT? It is important to recognize that the 20 Hz dielectric storage modulus shown in Figure 8 does not directly detect the initial dissolution of MMT molecules. To illustrate this, consider the initial transfer of MMT molecules into the MeAc liquid at a temperature not too far above the T_g value of MeAc. Depending upon the precise temperature, this might increase the 20 Hz storage modulus (because MMT molecules are now mobile enough to contribute) or decrease the 20 Hz storage modulus (because the addition of MMT molecules has slowed the reorientation rate of the MeAc molecules relative to 20 Hz).

An additional complication is that mixing within the MeAc-rich solution will be slowed by the addition of MMT (which increases the solution's T_g). This slow mixing might be the rate-limiting step for the overall process monitored by the 20 Hz storage modulus. We can make a plausibility argument for this scenario based upon a hypothetical isothermal experiment using a single-component glassformer and the dimensions of our bilayer sample. At T_g (i.e., $\tau_\alpha = 100$ s), the time required for a transformation front to move 200 nm through a moderately stable glass is about 2×10^5 s (assuming a molecular diameter of 1 nm and a transformation rate of 0.1 molecular diameter/τ_α).[45] The time required to uniformly mix a 400 nm layer via diffusion is about 8×10^6 s (assuming $D = 10^{-16}$ cm^2/s).[89] As the mixing time is much larger than the transformation time in this example, the stability of the starting glass would have little influence on an experimental observable that depends upon mixing after transformation.

There are possible applications where the dissolution rates of glasses of different stabilities could be important. For example, a stable glass of a pharmaceutical might be advantageous in order to inhibit crystallization.[90,91] Once inside the body, the dissolution rate of the glass is important.[12] For considering such applications, it would be useful to perform an experiment where the observable can be cleanly interpreted in terms of the concentration of the dissolved solute.

6. CONCLUSION

In this work, we used PVD to prepare codeposited glasses of methyl-*m*-toluate and methyl acetate, two molecular glassformers with an extremely high (50%) contrast in their T_g values. For all compositions, over a range of substrate temperatures, we observed a delayed return to the equilibrium liquid when the codeposited glasses were heated above the mixture T_g, as quantified by the onset temperature for the glass transition. When compared using normalized onset temperatures, the codeposited glasses have high kinetic stabilities that

https://doi.org/10.1021/acs.jpcb.5c01326
J. Phys. Chem. B 2025, 129, 6345−6356

are only slightly lower than those of PVD glasses of the pure components. These results are readily interpreted if we assume that the surface mobility of the two components is similar during codeposition, in spite of the large ratio of T_g values for the pure components. Additionally, we deposited bilayer samples of MMT and MeAc glasses and measured the rate at which the lower T_g component dissolved glasses of the high T_g component, for both highly stable and liquid-cooled glasses. For the dielectric observable with this sample geometry, glass stability has little impact on the rate of dissolution. Future experiments that cleanly separate the initial rate of dissolution from the subsequent mixing process would be useful.

■ ASSOCIATED CONTENT

Supporting Information

The Supporting Information is available free of charge at https://pubs.acs.org/doi/10.1021/acs.jpcb.5c01326.

Full dielectric spectra and VFT fitting parameters for bulk mixtures and a brief description of unusual crystallization time scales observed for layered films (PDF)

■ AUTHOR INFORMATION

Corresponding Author

Megan E. Tracy − *Department of Chemistry, University of Wisconsin-Madison, Madison, Wisconsin 53706, United States;* orcid.org/0000-0003-0824-431X; Email: megantracy88@gmail.com

Authors

Erik Thoms − *School of Molecular Sciences, Arizona State University, Tempe, Arizona 85287, United States;* orcid.org/0000-0002-2215-9974

Anthony Guiseppi-Elie − *Department of Electrical and Computer Engineering, Texas A&M University, College Station, Texas 77843, United States;* orcid.org/0000-0003-3218-9285

Ranko Richert − *School of Molecular Sciences, Arizona State University, Tempe, Arizona 85287, United States;* orcid.org/0000-0001-8503-3175

Mark D. Ediger − *Department of Chemistry, University of Wisconsin-Madison, Madison, Wisconsin 53706, United States;* orcid.org/0000-0003-4715-8473

Complete contact information is available at: https://pubs.acs.org/10.1021/acs.jpcb.5c01326

Notes

The authors declare no competing financial interest.

■ ACKNOWLEDGMENTS

We thank the U.S. National Science Foundation (CHE 2153944) for support of this work. We thank Christian Rodriguez-Tinoco and Lian Yu for useful discussions, and we thank Peter Harrowell for discussion of the results and for suggesting the study of glass dissolution. A.G.-E. acknowledges support via a TEES Research Professorship. We would also like to thank Bob Hamers for his guidance and assistance in establishing the deposition chambers in the Ediger lab, which allowed the further research leading to the present vapor-deposited glass project.

■ REFERENCES

(1) Lubchenko, V.; Wolynes, P. G. Theory of aging in structural glasses. *J. Chem. Phys.* **2004**, *121*, 2852−2865.

(2) Kasting, B. J.; Beasley, M. S.; Guiseppi-Elie, A.; Richert, R.; Ediger, M. D. Relationship between aged and vapor-deposited organic glasses: Secondary relaxations in methyl-m-toluate. *J. Chem. Phys.* **2019**, *151*, 144502.

(3) Zhang, Y.; Fakhraai, Z. Invariant Fast Diffusion on the Surfaces of Ultrastable and Aged Molecular Glasses. *Phys. Rev. Lett.* **2017**, *118*, 066101.

(4) Riechers, B.; Roed, L. A.; Mehri, S.; Ingebrigtsen, T. S.; Hecksher, T.; Dyre, J. C.; Niss, K. Predicting nonlinear physical aging of glasses from equilibrium relaxation via the material time. *Sci. Adv.* **2022**, *8*, No. eabl9809.

(5) Zhao, Y.; Shang, B.; Zhang, B.; Tong, X.; Ke, H.; Bai, H.; Wang, W. H. Ultrastable metallic glass by room temperature aging. *Sci. Adv.* **2022**, *8*, No. eabn3623.

(6) Esaki, Y.; Komino, T.; Matsushima, T.; Adachi, C. Enhanced Electrical Properties and Air Stability of Amorphous Organic Thin Films by Engineering Film Density. *J. Phys. Chem. Lett.* **2017**, *8*, 5891−5897.

(7) Frischeisen, J.; Yokoyama, D.; Endo, A.; Adachi, C.; Brütting, W. Increased light outcoupling efficiency in dye-doped small molecule organic light-emitting diodes with horizontally oriented emitters. *Org. Electron.* **2011**, *12*, 809−817.

(8) Rafols-Ribe, J.; Will, P. A.; Hanisch, C.; Gonzalez-Silveira, M.; Lenk, S.; Rodriguez-Viejo, J.; Reineke, S. High-performance organic light-emitting diodes comprising ultrastable glass layers. *Sci. Adv.* **2018**, *4*, No. eaar8332.

(9) Pandey, R.; Holmes, R. J. Graded donor-acceptor heterojunctions for efficient organic photovoltaic cells. *Adv. Mater.* **2010**, *22*, 5301−5305.

(10) Hedley, G. J.; Ruseckas, A.; Samuel, I. D. Light Harvesting for Organic Photovoltaics. *Chem. Rev.* **2017**, *117*, 796−837.

(11) Tenopala-Carmona, F.; Lee, O. S.; Crovini, E.; Neferu, A. M.; Murawski, C.; Olivier, Y.; Zysman-Colman, E.; Gather, M. C. Identification of the Key Parameters for Horizontal Transition Dipole Orientation in Fluorescent and TADF Organic Light-Emitting Diodes. *Adv. Mater.* **2021**, *33*, No. e2100677.

(12) Kawakami, K. Ultraslow Cooling for the Stabilization of Pharmaceutical Glasses. *J. Phys. Chem. B* **2019**, *123*, 4996−5003.

(13) Mehta, M.; Ragoonanan, V.; McKenna, G. B.; Suryanarayanan, R. Correlation between Molecular Mobility and Physical Stability in Pharmaceutical Glasses. *Mol. Pharmaceutics* **2016**, *13*, 1267−1277.

(14) Adrjanowicz, K.; Wojnarowska, Z.; Wlodarczyk, P.; Kaminski, K.; Paluch, M.; Mazgalski, J. Molecular mobility in liquid and glassy states of telmisartan (TEL) studied by broadband dielectric spectroscopy. *Eur. J. Pharm. Sci.* **2009**, *38*, 395−404.

(15) Adrjanowicz, K.; Paluch, M.; Ngai, K. L. Determining the structural relaxation times deep in the glassy state of the pharmaceutical Telmisartan. *J. Phys.: Condens. Matter* **2010**, *22*, 125902.

(16) Kissi, E. O.; Grohganz, H.; Lobmann, K.; Ruggiero, M. T.; Zeitler, J. A.; Rades, T. Glass-Transition Temperature of the beta-Relaxation as the Major Predictive Parameter for Recrystallization of Neat Amorphous Drugs. *J. Phys. Chem. B* **2018**, *122*, 2803−2808.

(17) Qiu, Y.; Bieser, M. E.; Ediger, M. D. Dense Glass Packing Can Slow Reactions with an Atmospheric Gas. *J. Phys. Chem. B* **2019**, *123*, 10124−10130.

(18) Viciosa, M. T.; Moura Ramos, J. J.; Diogo, H. P. Thermal behavior and molecular mobility studies in the supercooled liquid and glassy states of carvedilol and loratadine. *Int. J. Pharm.* **2020**, *584*, 119410.

(19) Beasley, M. S.; Bishop, C.; Kasting, B. J.; Ediger, M. D. Vapor-Deposited Ethylbenzene Glasses Approach "Ideal Glass. *Density J. Phys. Chem. Lett.* **2019**, *10*, 4069−4075.

(20) El Banna, A. A.; McKenna, G. B. Challenging the Kauzmann paradox using an ultra-stable perfluoropolymer glass with a fictive

temperature below the dynamic VFT temperature. *Sci. Rep.* **2023**, *13*, 4224.
(21) Kearns, K. L.; Swallen, S. F.; Ediger, M. D.; Wu, T.; Sun, Y.; Yu, L. Hiking down the energy landscape: Progress toward the Kauzmann temperature via vapor deposition. *J. Phys. Chem. B* **2008**, *112*, 4934−4942.
(22) Stillinger, F. H.; Debenedetti, P. G.; Truskett, T. M. The Kauzmann Paradox Revisited†. *J. Phys. Chem. B* **2001**, *105*, 11809−11816.
(23) Kong, D.; Meng, Y.; McKenna, G. B. Searching for the ideal glass transition: Going to yotta seconds and beyond. *J. Non-Cryst. Solids* **2023**, *606*, 122186.
(24) McKenna, G. B.; Zhao, J. Accumulating evidence for non-diverging time-scales in glass-forming fluids. *J. Non-Cryst. Solids* **2015**, *407*, 3−13.
(25) Guiselin, B.; Tarjus, G.; Berthier, L. *Is glass a state of matter?* Physics and Chemistry of Glasses. *Eur. J. Glass Sci. Technol., Part B* **2022**, *63*, 136−144.
(26) Duval, E.; Saviot, L.; David, L.; Etienne, S.; Jal, J. F. Effect of physical aging on the low-frequency vibrational density of states of a glassy polymer. *Europhys. Lett.* **2003**, *63*, 778−784.
(27) Berthier, L.; Ediger, M. D. How to "measure" a structural relaxation time that is too long to be measured? *J. Chem. Phys.* **2020**, *153*, 044501.
(28) Swallen, S. F.; Kearns, K. L.; Mapes, M. K.; Kim, Y. S.; McMahon, R. J.; Ediger, M. D.; Wu, T.; Yu, L.; Satija, S. Organic glasses with exceptional thermodynamic and kinetic stability. *Science* **2007**, *315*, 353−356.
(29) Berthier, L.; Charbonneau, P.; Flenner, E.; Zamponi, F. Origin of Ultrastability in Vapor-Deposited Glasses. *Phys. Rev. Lett.* **2017**, *119*, 188002.
(30) Chai, Y.; Salez, T.; McGraw, J. D.; Benzaquen, M.; Dalnoki-Veress, K.; Raphael, E.; Forrest, J. A. A direct quantitative measure of surface mobility in a glassy polymer. *Science* **2014**, *343*, 994−999.
(31) Chen, Y.; Zhu, M.; Laventure, A.; Lebel, O.; Ediger, M. D.; Yu, L. Influence of Hydrogen Bonding on the Surface Diffusion of Molecular Glasses: Comparison of Three Triazines. *J. Phys. Chem. B* **2017**, *121*, 7221−7227.
(32) Fakhraai, Z.; Forrest, J. A. Measuring the surface dynamics of glassy polymers. *Science* **2008**, *319*, 600−604.
(33) Roth, C. B.; McNerny, K. L.; Jager, W. F.; Torkelson, J. M. Eliminating the Enhanced Mobility at the Free Surface of Polystyrene: Fluorescence Studies of the Glass Transition Temperature in Thin Bilayer Films of Immiscible Polymers. *Macromolecules* **2007**, *40*, 2568−2574.
(34) Ruan, S.; Zhang, W.; Sun, Y.; Ediger, M. D.; Yu, L. Surface diffusion and surface crystal growth of tris-naphthyl benzene glasses. *J. Chem. Phys.* **2016**, *145*, 064503.
(35) Stevenson, J. D.; Wolynes, P. G. On the surface of glasses. *J. Chem. Phys.* **2008**, *129*, 234514.
(36) Thoms, E.; Gabriel, J. P.; Guiseppi-Elie, A.; Ediger, M. D.; Richert, R. In situ observation of fast surface dynamics during the vapor-deposition of a stable organic glass. *Soft Matter.* **2020**, *16*, 10860−10864.
(37) Tylinski, M.; Beasley, M. S.; Chua, Y. Z.; Schick, C.; Ediger, M. D. Limited surface mobility inhibits stable glass formation for 2-ethyl-1-hexanol. *J. Chem. Phys.* **2017**, *146*, 203317.
(38) Chen, Y.; Zhang, W.; Yu, L. Hydrogen Bonding Slows Down Surface Diffusion. *J. Phys. Chem. B* **2016**, *120*, 8007−8015.
(39) Zhang, W.; Brian, C. W.; Yu, L. Fast surface diffusion of amorphous o-terphenyl and its competition with viscous flow in surface evolution. *J. Phys. Chem. B* **2015**, *119*, 5071−5078.
(40) Zhang, Y.; Fakhraai, Z. Decoupling of surface diffusion and relaxation dynamics of molecular glasses. *Proc. Natl. Acad. Sci. U. S. A.* **2017**, *114*, 4915−4919.
(41) Zhang, Y.; Potter, R.; Zhang, W.; Fakhraai, Z. Using tobacco mosaic virus to probe enhanced surface diffusion of molecular glasses. *Soft Matter.* **2016**, *12*, 9115−9120.
(42) Zhu, L.; Brian, C. W.; Swallen, S. F.; Straus, P. T.; Ediger, M. D.; Yu, L. Surface self-diffusion of an organic glass. *Phys. Rev. Lett.* **2011**, *106*, 256103.
(43) Ediger, M. D.; Gruebele, M.; Lubchenko, V.; Wolynes, P. G. Glass Dynamics Deep in the Energy Landscape. *J. Phys. Chem. B* **2021**, *125*, 9052−9068.
(44) Dalal, S. S.; Walters, D. M.; Lyubimov, I.; de Pablo, J. J.; Ediger, M. D. Tunable molecular orientation and elevated thermal stability of vapor-deposited organic semiconductors. *Proc. Natl. Acad. Sci. U. S. A.* **2015**, *112*, 4227−4232.
(45) Tylinski, M.; Sepulveda, A.; Walters, D. M.; Chua, Y. Z.; Schick, C.; Ediger, M. D. Vapor-deposited glasses of methyl-m-toluate: How uniform is stable glass transformation? *J. Chem. Phys.* **2015**, *143*, 244509.
(46) Walters, D. M.; Antony, L.; de Pablo, J. J.; Ediger, M. D. Influence of Molecular Shape on the Thermal Stability and Molecular Orientation of Vapor-Deposited Organic Semiconductors. *J. Phys. Chem. Lett.* **2017**, *8*, 3380−3386.
(47) Beasley, M. S.; Kasting, B. J.; Tracy, M. E.; Guiseppi-Elie, A.; Richert, R.; Ediger, M. D. Physical vapor deposition of a polyamorphic system: Triphenyl phosphite. *J. Chem. Phys.* **2020**, *153*, 124511.
(48) Kasting, B. J.; Gabriel, J. P.; Tracy, M. E.; Guiseppi-Elie, A.; Richert, R.; Ediger, M. D. Unusual Transformation of Mixed Isomer Decahydroisoquinoline Stable Glasses. *J. Phys. Chem. B* **2023**, *127*, 5948−5958.
(49) Swallen, S. F.; Traynor, K.; McMahon, R. J.; Ediger, M. D.; Mates, T. E. Stable glass transformation to supercooled liquid via surface-initiated growth front. *Phys. Rev. Lett.* **2009**, *102*, 065503.
(50) Sepulveda, A.; Tylinski, M.; Guiseppi-Elie, A.; Richert, R.; Ediger, M. D. Role of fragility in the formation of highly stable organic glasses. *Phys. Rev. Lett.* **2014**, *113*, 045901.
(51) Rafols-Ribe, J.; Gonzalez-Silveira, M.; Rodriguez-Tinoco, C.; Rodriguez-Viejo, J. The role of thermodynamic stability in the characteristics of the devitrification front of vapour-deposited glasses of toluene. *Phys. Chem. Chem. Phys.* **2017**, *19*, 11089−11097.
(52) Whitaker, K. R.; Ahrenberg, M.; Schick, C.; Ediger, M. D. *Vapor-deposited alpha,alpha*, beta-tris-naphthylbenzene glasses with low heat capacity and high kinetic stability. *J. Chem. Phys.* **2012**, *137*, 154502.
(53) Vila-Costa, A.; Gonzalez-Silveira, M.; Rodríguez-Tinoco, C.; Rodríguez-López, M.; Rodriguez-Viejo, J. Emergence of equilibrated liquid regions within the glass. *Nat. Phys.* **2023**, *19*, 114−119.
(54) Ruiz-Ruiz, M.; Vila-Costa, A.; Bar, T.; Rodríguez-Tinoco, C.; Gonzalez-Silveira, M.; Plaza, J. A.; Alcalá, J.; Fraxedas, J.; Rodriguez-Viejo, J. Real-time microscopy of the relaxation of a glass. *Nat. Phys.* **2023**, *19*, 1509−1515.
(55) Herrero, C.; Scalliet, C.; Ediger, M. D.; Berthier, L. Two-step devitrification of ultrastable glasses. *Proc. Natl. Acad. Sci. U. S. A.* **2023**, *120*, No. e2220824120.
(56) Herrero, C.; Ediger, M. D.; Berthier, L. Front propagation in ultrastable glasses is dynamically heterogeneous. *J. Chem. Phys.* **2023**, *159*, 114504.
(57) Qiu, Y.; Antony, L. W.; de Pablo, J. J.; Ediger, M. D. Photostability Can Be Significantly Modulated by Molecular Packing in Glasses. *J. Am. Chem. Soc.* **2016**, *138*, 11282−11289.
(58) Qiu, Y.; Antony, L. W.; Torkelson, J. M.; de Pablo, J. J.; Ediger, M. D. Tenfold increase in the photostability of an azobenzene guest in vapor-deposited glass mixtures. *J. Chem. Phys.* **2018**, *149*, 204503.
(59) Smith, R. S.; May, R. A.; Kay, B. D. Probing Toluene and Ethylbenzene Stable Glass Formation Using Inert Gas Permeation. *J. Phys. Chem. Lett.* **2015**, *6*, 3639−3644.
(60) Pakhomenko, E.; He, S.; Holmes, R. J. Polarization-Induced Exciton−Polaron Quenching in Organic Light-Emitting Devices and Its Control by Dipolar Doping. *Adv. Opt. Mater.* **2022**, *10*, 2201348.
(61) Cheng, S.; Lee, Y.; Yu, J.; Yu, L.; Ediger, M. D. Surface Equilibration Mechanism Controls the Stability of a Model Codeposited Glass Mixture of Organic Semiconductors. *J. Phys. Chem. Lett.* **2023**, *14*, 4297−4303.

https://doi.org/10.1021/acs.jpcb.5c01326
J. Phys. Chem. B 2025, 129, 6345−6356

(62) Cheng, S.; Lee, Y.; Yu, J.; Yu, L.; Ediger, M. D. Generic Behavior of Ultrastability and Anisotropic Molecular Packing in Codeposited Organic Semiconductor Glass Mixtures. *Chem. Mater.* **2024**, *36*, 3205−3214.
(63) Jiang, J.; Walters, D. M.; Zhou, D.; Ediger, M. D. Substrate temperature controls molecular orientation in two-component vapor-deposited glasses. *Soft Matter.* **2016**, *12*, 3265−3270.
(64) Whitaker, K. R.; Scifo, D. J.; Ediger, M. D.; Ahrenberg, M.; Schick, C. Highly stable glasses of cis-decalin and cis/trans-decalin mixtures. *J. Phys. Chem. B* **2013**, *117*, 12724−12733.
(65) Korber, T.; Minikejew, R.; Potzschner, B.; Bock, D.; Rossler, E. A. Dynamically asymmetric binary glass formers studied by dielectric and NMR spectroscopy. *Eur. Phys. J. E* **2019**, *42*, 143.
(66) Korber, T.; Krohn, F.; Neuber, C.; Schmidt, H. W.; Rossler, E. A. Reorientational dynamics of highly asymmetric binary non-polymeric mixtures - a dielectric spectroscopy study. *Phys. Chem. Chem. Phys.* **2021**, *23*, 7200−7212.
(67) Korber, T.; Potzschner, B.; Krohn, F.; Rossler, E. A. Reorientational dynamics in highly asymmetric binary low-molecular mixtures-A quantitative comparison of dielectric and NMR spectroscopy results. *J. Chem. Phys.* **2021**, *155*, 024504.
(68) Tracy, M. E.; Kasting, B. J.; Herrero, C.; Berthier, L.; Richert, R.; Guiseppi-Elie, A.; Ediger, M. D. Initial stages of rejuvenation of vapor-deposited glasses during isothermal annealing: Contrast between experiment and simulation. *J. Chem. Phys.* **2024**, *161*, 224504.
(69) Tylinski, M.; Chua, Y. Z.; Beasley, M. S.; Schick, C.; Ediger, M. D. Vapor-deposited alcohol glasses reveal a wide range of kinetic stability. *J. Chem. Phys.* **2016**, *145*, 174506.
(70) Beasley, M. S.; Tylinski, M.; Chua, Y. Z.; Schick, C.; Ediger, M. D. Glasses of three alkyl phosphates show a range of kinetic stabilities when prepared by physical vapor deposition. *J. Chem. Phys.* **2018**, *148*, 174503.
(71) Chen, Z.; Zhao, Y.; Wang, L. M. Enthalpy and dielectric relaxations in supercooled methyl m-toluate. *J. Chem. Phys.* **2009**, *130*, 204515.
(72) Richert, R. A simple current-to-voltage interface for dielectric relaxation measurements in the range 10^{-3} to 10^{7} Hz. *Rev. Sci. Instrum.* **1996**, *67*, 3217−3221.
(73) Singh, L. P.; Richert, R. Two-channel impedance spectroscopy for the simultaneous measurement of two samples. *Rev. Sci. Instrum.* **2012**, *83*, 033903.
(74) Gordon, M.; Taylor, J. S. Ideal copolymers and the second-order transitions of synthetic rubbers. i. non-crystalline copolymers. *J. Appl. Chem.* **1952**, *2*, 493−500.
(75) Chua, Y. Z.; Ahrenberg, M.; Tylinski, M.; Ediger, M. D.; Schick, C. How much time is needed to form a kinetically stable glass? AC calorimetric study of vapor-deposited glasses of ethylcyclohexane. *J. Chem. Phys.* **2015**, *142*, 054506.
(76) Kearns, K. L.; Krzyskowski, P.; Devereaux, Z. Using deposition rate to increase the thermal and kinetic stability of vapor-deposited hole transport layer glasses via a simple sublimation apparatus. *J. Chem. Phys.* **2017**, *146*, 203328.
(77) Chacko, R. N.; Landes, F. P.; Biroli, G.; Dauchot, O.; Liu, A. J.; Reichman, D. R. Dynamical Facilitation Governs the Equilibration Dynamics of Glasses. *Phys. Rev. X* **2024**, *14*, 031012.
(78) Rodriguez-Tinoco, C.; Gonzalez-Silveira, M.; Rafols-Ribe, J.; Vila-Costa, A.; Martinez-Garcia, J. C.; Rodriguez-Viejo, J. Surface-Bulk Interplay in Vapor-Deposited Glasses: Crossover Length and the Origin of Front Transformation. *Phys. Rev. Lett.* **2019**, *123*, 155501.
(79) Flenner, E.; Berthier, L.; Charbonneau, P.; Fullerton, C. J. Front-Mediated Melting of Isotropic Ultrastable Glasses. *Phys. Rev. Lett.* **2019**, *123*, 175501.
(80) Dawson, K. J.; Zhu, L.; Yu, L.; Ediger, M. D. Anisotropic structure and transformation kinetics of vapor-deposited indomethacin glasses. *J. Phys. Chem. B* **2011**, *115*, 455−463.
(81) Chen, Z.; Sepulveda, A.; Ediger, M. D.; Richert, R. Dynamics of glass-forming liquids. XVI. Observation of ultrastable glass transformation via dielectric spectroscopy. *J. Chem. Phys.* **2013**, *138*, 12A519.
(82) Walters, D. M.; Richert, R.; Ediger, M. D. Thermal stability of vapor-deposited stable glasses of an organic semiconductor. *J. Chem. Phys.* **2015**, *142*, 134504.
(83) Vila-Costa, A.; Rafols-Ribe, J.; Gonzalez-Silveira, M.; Lopeandia, A. F.; Abad-Munoz, L.; Rodriguez-Viejo, J. Nucleation and Growth of the Supercooled Liquid Phase Control Glass Transition in Bulk Ultrastable Glasses. *Phys. Rev. Lett.* **2020**, *124*, 076002.
(84) Sepulveda, A.; Swallen, S. F.; Ediger, M. D. Manipulating the properties of stable organic glasses using kinetic facilitation. *J. Chem. Phys.* **2013**, *138*, 12A517.
(85) Kearns, K. L.; Ediger, M. D.; Huth, H.; Schick, C. One Micrometer Length Scale Controls Kinetic Stability of Low-Energy Glasses. *J. Phys. Chem. Lett.* **2010**, *1*, 388−392.
(86) Avrami, M. Kinetics of Phase ChangeI General Theory. *J. Chem. Phys.* **1939**, *7*, 1103−1112.
(87) Lee, Y.; Cheng, S.; Ediger, M. D. High Density Two-Component Glasses of Organic Semiconductors Prepared by Physical Vapor Deposition. *J. Phys. Chem. Lett.* **2024**, *15*, 8085−8092.
(88) Wolynes, P. G. Spatiotemporal structures in aging and rejuvenating glasses. *Proc. Natl. Acad. Sci. U. S. A.* **2009**, *106*, 1353−1358.
(89) Swallen, S. F.; Ediger, M. D. Self-diffusion of the amorphous pharmaceutical indomethacin near Tg. *Soft Matter.* **2011**, *7*, 10339−10344.
(90) Bagchi, K.; Fiori, M. E.; Bishop, C.; Toney, M. F.; Ediger, M. D. Stable Glasses of Organic Semiconductor Resist Crystallization. *J. Phys. Chem. B* **2021**, *125*, 461−466.
(91) Rodríguez-Tinoco, C.; Gonzalez-Silveira, M.; Ràfols-Ribé, J.; Garcia, G.; Rodríguez-Viejo, J. Highly stable glasses of celecoxib: Influence on thermo-kinetic properties, microstructure and response towards crystal growth. *J. Non-Cryst. Solids* **2015**, *407*, 256−261.

https://doi.org/10.1021/acs.jpcb.5c01326
J. Phys. Chem. B 2025, 129, 6345−6356